**Atmospheric
Chemistry
and Physics
Discussions**

A reanalysis of MODIS fine mode fraction over ocean using OMI and daily GOCART simulations

T. A. Jones[1,3] **and S. A. Christopher**[1,2]

[1]Earth System Science Center, UAHuntsville, Huntsville, AL, USA
[2]Department of Atmospheric Sciences, UAHuntsville, Huntsville, AL, USA
[3]Cooperative Institute for Mesoscale Meteorological Studies, Norman, OK, USA

Correspondence to: T. A. Jones (thomas.jones@noaa.gov)

ACPD

10, 29773–29807, 2010

A reanalysis of MODIS fine mode fraction over ocean

T. A. Jones and
S. A. Christopher

Title Page

Abstract	Introduction
Conclusions	References
Tables	Figures

|◄ | ►|

◄ | ►

Back | Close

Full Screen / Esc

Printer-friendly Version

Interactive Discussion

Abstract

Using daily Goddard Chemistry Aerosol Radiation and Transport (GOCART) model simulations and columnar retrievals of 0.55 μm aerosol optical thickness (AOT) and fine mode fraction (FMF) from the Moderate Resolution Imaging Spectroradiometer (MODIS), we estimate the aerosol concentration and particle size over the global oceans between June 2006 and May 2007 due to black carbon (BC), organic carbon (OC), dust (DU), sea-salt (SS), and sulfate (SU) components. Using Aqua-MODIS aerosol properties embedded in the CERES-SSF product, we find that the mean MODIS FMF values are SS: 0.31±0.09, DU: 0.49±0.13, SU: 0.77±0.16, and (BC+OC):0.80±0.16. We further combine information from the ultraviolet spectrum using the Ozone Monitoring Instrument (OMI) onboard the Aura satellite to improve the classification process, since dust and carbonaceous aerosols have positive Aerosol Index (AI) values >0.5 while other aerosol types have near zero values. By combining MODIS and OMI datasets, we were able to identify and remove data in the SU and CC regions that were not associated with those aerosol types.

The same methods used to estimate aerosol size characteristics from MODIS data within the CERES-SSF product were also applied to Level 2 (L2) MODIS aerosol data from both Terra and Aqua satellites for the same time period. As expected, FMF estimates from L2 Aqua data agreed well with the CERES-SSF dataset, also from Aqua. However, the FMF estimate for DU from Terra data was significantly lower (0.37 vs. 0.49) indicating that sensor calibration, sampling differences and/or diurnal changes in DU aerosol size characteristics were occurring. Differences for other aerosol types were generally smaller. Sensitivity studies show that a difference of 0.1 in the estimate of the anthropogenic component of FMF produces a corresponding change of 0.2 in the anthropogenic component of AOT (assuming a unit value of AOT). This uncertainty would then be passed along to any satellite-derived estimates of anthropogenic aerosol radiative effects.

**A reanalysis of
MODIS fine mode
fraction over ocean**

T. A. Jones and
S. A. Christopher

1 Introduction

Satellite remote sensing has provided many important insights into the global distribution of aerosols, their properties, and how they modify the earth-atmosphere system through various effects (e.g., Yu et al., 2006). In particular, multi-spectral data from the Moderate Resolution Imaging Spectroradiometer (MODIS) onboard both the Terra and Aqua satellites have provided valuable information for assessing aerosol characteristics beyond just retrieved total column 0.55 µm aerosol optical thickness (AOT) (e.g., Jones and Christopher, 2007a). While the MODIS cannot directly provide aerosol speciation, fine mode fraction (FMF), which represents the ratio of fine mode AOT (r_e<0.25 µm) to the total AOT, has often been used as a proxy for separating anthropogenic from natural aerosols (Bellouin, 2005, 2008; Kaufman et al., 2005a,b; Christopher et al., 2006; Jones and Christopher, 2007a; Yu et al., 2009). Aerosols such as sulfates (SU) and carbonates (black carbon and organic carbon) (CC) are predominately fine mode in nature producing high FMF values, whereas mechanically-produced dust (DU) and sea-salt (SS) aerosols are larger (coarse mode) resulting in lower FMF values (Kaufman et al., 2005a,b). Additional sensors onboard other satellites can provide value-added information over what is available from MODIS alone. For example, the Ozone Monitoring Instrument (OMI) onboard the Aura satellite collects data in the ultraviolet (UV) spectrum, which is sensitive to UV-absorbing aerosols and their elevation (Torres et al., 2007). UV-absorbing aerosols include both elevated dust and black carbon, whereas sulfates and sea-salt are not. Using a combination of these data in conjunction with GOCART simulated aerosols, we estimate satellite-derived columnar aerosol properties for various aerosol types in both space and time. This distinction is important since different aerosol types can produce different radiative effects (Christopher and Jones, 2008a).

The primary objective of this study is to present a follow-up to the analysis first discussed by Jones and Christopher (2007a) (hereafter JC07). In JC07, MODIS FMF, TOMS Aerosol Index (AI), and MOPITT Carbon Monoxide (CO) retrievals were

A reanalysis of MODIS fine mode fraction over ocean

T. A. Jones and
S. A. Christopher

combined with GOCART simulations (Chin et al., 2002, 2004) to assess the concentration, size, and vertical distribution of SS, DU, and anthropogenic (AN) aerosols. Previous research (Kaufman et al., 2005a,b; Bellouin et al., 2005, 2008) and more recently Yu et al. (2009) have also employed similar techniques to classify aerosols through MODIS AOT and FMF. The average MODIS FMF values from various studies are summarized in Table 1. Their results clearly show anthropogenic aerosols are mostly fine mode whereas mechanically produced aerosols such as DU and SS are predominantly coarse mode. We use the term "predominantly" to note that sea salt and dust is not devoid of fine mode and neither is smoke and sulfate completely devoid of coarse mode aerosols. However, significant differences in FMF estimates remain between studies, especially when it comes to SS and AN (Yu et al., 2009). Using additional data sources such as TOMS-AI, JC07 attempted to reduce these uncertainties, but were only partially successful owing to several limitations.

This study reexamines these questions using improved methods, updated datasets, and multi-dataset comparisons that are combined to produce a more accurate picture satellite-retrieved aerosol properties. GOCART aerosol simulations are used in this study at a daily resolution compared to monthly resolution available for JC07. Given that the MODIS aerosol properties were not available for every day during a particular month, we were required to make the assumption in JC07 that available data represented an adequate measure of the monthly average. The GOCART model also provides information of the vertical distribution of aerosols and aerosol size characteristics, which is now incorporated into the analysis (Chin et al., 2003). Thus, we can now assess the importance of aerosol height on aerosol classification techniques, which will be vital for future research as more observations of aerosol vertical profiles become available (e.g. CALIPSO). We also replace TOMS-AI with OMI-AI since the latter is available at a higher resolution and at nearly the same time as the Aqua MODIS data. Finally, we perform this analysis for three separate satellite datasets to assess the importance of instrument calibration, sampling, and diurnal variability to the retrieved properties of individual aerosol types. Using these methods, the impacts of

these differences on component aerosol radiative effects can be estimated, providing an important assessment tool when considering the relative impacts of different aerosol types to the climate.

2 Data

2.1 CERES-SSF (Aqua)

Total and fine-mode AOT from MODIS are first obtained over the global oceans from the Collection 5 aerosol retrievals contained within the Clouds and the Earth's Radiant Energy System Single Scanner Footprint (CERES-SSF) product (Loeb and Manalo-Smith, 2005) between June 2006 and May 2007 from the Aqua satellite. Aqua is a polar orbiting satellite with an equatorial overpass time of approximately 13:30 p.m. LT (early afternoon) on which both CERES and MODIS are located. The CERES instrument measures broadband radiances at the top of the atmosphere (TOA) that are converted into fluxes using angular dependence models (ADMs) developed by Zhang et al. (2005). These models use observed radiances combined with satellite viewing geometry, atmospheric conditions, and MODIS aerosol properties to derive TOA fluxes in cloud free environments. The CERES-SSF product combines measurements from the CERES instrument with those from the MODIS on the same satellite using a point-spread function (PSF) to apply appropriate weights to the 10 km resolution MODIS Collection 5 AOT within each 20 km CERES footprint. This product has been used extensively for studying aerosol forcing (e.g., Christopher et al., 2006).

2.2 MODIS (Terra and Aqua)

Aerosol properties are also derived from the Level-2 (L2), Collection 5 Terra (MOD04) and Aqua (MYD04) products for the same time period to compare against the MODIS values contained within the Aqua CERES-SSF dataset. While the aerosol products in

A reanalysis of MODIS fine mode fraction over ocean

T. A. Jones and
S. A. Christopher

the CERES-SSF files are reported at the CERES instrument resolution of 20 km, the raw MODIS L2 AOT data are available at a higher 10 km resolution. Over the ocean, the AOT uncertainty is given as $\tau=0.03\pm0.05\tau$, with FMF uncertainty on the order of 30% (Remer et al., 2005). The greatest uncertainties in τ and FMF occur when aerosol

5   concentrations are low ($\tau<0.1$), such as the case for sea-salt aerosols over otherwise clean ocean conditions (e.g., Kleidman et al., 2005). When aerosol concentrations are low, the differences in reflectances between bands necessary to retrieve aerosol size information become comparable with the uncertainties in reflectance measurements. When studying the size properties of aerosol in these conditions, the uncertainties must

10 be made note of. Additional uncertainties in aerosol retrievals arise from the effects of nearby clouds (Zhang and Reid, 2006). To reduce these uncertainties, we remove all pixels where MODIS cloud fraction is greater than 30% (Gupta and Christopher, 2007). Comparing MODIS cloud fraction with FMF also showed that FMF does not appear to change significantly as a function of cloud fraction for most regions over the ocean until

15 cloud fraction exceeds at least 50% (Jones et al., 2009).

Since the AOT in the CERES-SSF is derived from the Level 2 MODIS data, it is expected that both datasets (CERES-SSF AOT and MODIS L2 AOT) should report similar statistics although the CERES-SSF convolves the MODIS AOT based on the point-spread functions. However, using the larger CERES footprint requires the use

20 of cloud clearing thresholds over a larger area, introducing a "clear-sky" bias to the data (Christopher and Jones, 2008b). The result of the bias is for AOT reported by the CERES-SSF product to be underestimated compared to MODIS L2 AOT in regions where significant cloud cover is often present. Whether or not this bias translates into a difference in retrieved aerosol size characteristics will be examined as part of this

25 study.

MODIS L2 data from the Terra satellite (MOD04) were also acquired and analyzed to determine if either instrument biases or diurnal changes in aerosol properties produce a measurable impact on observed aerosol size distributions. The Terra satellite is also a polar orbiter, but has an equatorial overpass time of approximately 10:30 a.m. LT,

A reanalysis of
MODIS fine mode
fraction over ocean

T. A. Jones and
S. A. Christopher

Title Page

Abstract | Introduction

Conclusions | References

Tables | Figures

◄ | ►

◄ | ►

Back | Close

Full Screen / Esc

Printer-friendly Version

Interactive Discussion

or ∼3 h before Aqua. Total aerosol concentrations are expected to be similar to Aqua observations, though Remer et al. (2008) noted an unexplained offset of 0.015 between Terra and Aqua AOT retrievals. The 3 h difference in observation time between Terra and Aqua may also produce different results in certain regions due to diurnal variability in aerosol concentrations, cloud cover, humidity, and sampling (e.g., Smirnov et al., 2002; Wang et al., 2004).

2.3 OMI-AI

The UV Aerosol Index (AI) from the Ozone Monitoring Instrument (OMI) on the Aura satellite, which has an equatorial overpass time of about 13:45 p.m. LT similar to that of Aqua, is used to assess UV-absorbing aerosols such as mineral dust. At nadir, the OMI pixel resolution is 13×24 km. We use Level-2, Collection 3 AI which represents the difference in wavelength dependence of reflected radiation at 342.5 and 388 nm compared to a pure molecular (Rayleigh scattering) background (Torres et al., 2007). Large concentrations of DU or BC aerosols exhibit positive AI values whereas SU and SS have AI values near zero, or slightly negative. Torres et al. (1998, 2002), Hsu et al. (1999), and Ginoux and Torres (2003) all noted an important sensitivity to UV-absorbing aerosols as a function of height. For a given aerosol concentration, OMI-AI will be larger the higher in the atmosphere the aerosols exist. This sensitivity does not extend to non-absorbing aerosols. The sensitivity of OMI-AI to both aerosol type and height makes it useful for satellite-derived aerosol classification techniques. To account for sub-pixel cloud contamination, AI pixels whose quality flags indicate the presence of clouds are removed from consideration.

2.4 GOCART

Since MODIS and OMI cannot separate each pixel into speciated components a-priori, we use GOCART model simulations to estimate the aerosol composition (Chin et al., 2002, 2004). GOCART simulates global distributions of BC, OC, SU, DU, and SS

A reanalysis of MODIS fine mode fraction over ocean

T. A. Jones and
S. A. Christopher

Full Screen / Esc

Printer-friendly Version

Interactive Discussion

aerosols. These simulations are used to determine aerosol speciation since we are updating a previous study that uses GOCART (JC07) and since it was made readily available. This model uses global emissions of aerosols and precursor gases from anthropogenic, natural, and biomass burning sources, and includes transport and removal

5 processes that are driven by assimilated meteorological fields. The simulated mass loadings of each aerosol species are then converted to AOT using mass extinction coefficients assuming external mixing and spherical particles. See Chin et al. (2002, 2004, 2009) for further details. Aerosol products modeled by GOCART are produced with a spatial resolution of 2.5°×2.0°, with daily averaged data used in this research.

10 GOCART defines FMF as the ratio of the sum of the optical depths from SU, BC, and OC (which are assumed to be 100% fine mode, $r_e < 0.5\,\mu m$), and fine mode components of DU and SS ($r_e < 1.0\,\mu m$) to the total AOT. For hygroscopic aerosols (i.e. all types except dust), aerosol size is also dependent on surrounding atmospheric humidity with aerosols increasing in size for more humid environments (Chin et al., 2002).

15 The naturally occurring and anthropogenic components of SU, OC, and BC are also simulated by GOCART, providing the opportunity for more in-depth analysis of these aerosol types. In particular, a significant amount of SU in the atmosphere originates from volcanic emissions and to a lesser extent, dimethylsulfide (DMS) (Chin et al., 2009). On average, 20% of the total SU component of AOT is assumed to be from

20 natural sources (Chin et al., 2002). The naturally occurring component of OC from biomass burning is also considered, but only contributes less than 10% to the total OC component of AOT. In addition, the naturally occurring component of BC is assumed to be zero. As a result, we do not discriminate between natural and anthropogenic carbonaceous aerosols for the remainder of this research. Finally, GOCART provides

25 vertical distributions of each aerosol species based on source region and atmospheric transport (Chin et al., 2007).

While GOCART has been thoroughly validated over the years (e.g., Chin et al., 2009), significant assumptions and uncertainties remain present that could cause errors when computing individual aerosol type regions. One important assumption made

by GOCART is that aerosols are externally mixed. This means that aerosols do not chemically react or otherwise combine with on another. This is not always the case as internal mixing often occurs and can take the form of sulfate coated dust aerosols (Levin et al., 1996) and/or black carbon (Seland et al., 2008). Under these circum-
5 stances, the GOCART aerosol species computations may not be accurate; however, Chin et al. (2002) assumed that this uncertainty should be small.

Another important factor to consider is the accuracy of the GOCART model at estimating aerosol concentration and speciation characteristics compared to other models and methods. Textor et al. (2006) studied this question in detail and found a reason-
10 ably good agreement in the distribution of individual aerosol types from over a dozen different models. However, significant differences in aerosol mass-loadings simulated by individual models were found for DU and especially SS aerosol types. In particular, the SS mass loadings vary at least ±50% when all models are considered. These variations were deemed to be primarily due to differences in the particle size distributions
15 and source fluxes assumed by each model. Furthermore, DU and SS concentrations are also highly dependent on assumed atmospheric conditions, especially wind speed. The sources for the atmospheric parameters assimilated into individual models varies from observations, to numerical model analysis, to long term climate averages, which combined with resolution differences can produce very different SS and DU production
20 and transport characteristics. Since this study focuses on ocean regions only, the uncertainty in SS concentrations is a primary concern as we are using a threshold-based approach to determine aerosol type regions as done in JC07. When considering OC, BC, and SU aerosols, much greater agreement exists be modeled mass-loadings as similar datasets are employed to estimate their spatial and temporal emission charac-
25 teristics (Textor et al., 2006).

3   Methodology

The methodology used here closely follows that of JC07 where the swath-level aerosol (CERES-SSF and MODIS L2) and OMI-AI data are aggregated to the 2.0×2.5° resolution corresponding to GOCART simulated products. For all satellite data, pixels with solar and/or viewing zenith angles greater than ±60° are removed due to increasing uncertainties and pixel sizes as these extreme angles. Using this threshold does have the impact of reducing sampling in high latitude regions during certain seasons. Regions corresponding to a single aerosol type are defined as those where at least 80% of the total GOCART simulated AOT for a particular grid cell is accounted for by that aerosol type. The daily mean MODIS AOT and FMF values within that grid cell are compared with GOCART simulations. This is different than the method employed by Yu et al. (2009) where specific geographical regions based on those defined by Kaufman et al. (2005a) were chosen and assumed to be representative of a single aerosol type. An additional requirement that MODIS AOT be less than 0.1 for SS aerosols is also included to remove possible cloud contamination noted in the Southern Hemisphere (Zhang and Reid, 2006). This analysis is performed globally for each day; thus, regions of a specific aerosol type are allowed to move and change in size as a function of space and time. Corresponding probability distributions are also shown to estimate the uncertainty in these statistics as well as to compare the GOCART values to the satellite retrievals.

As in JC07, we compare regions of anthropogenic vs. naturally occurring SU aerosols, although we note that some uncertainly exists in this distinction. When comparing statistics with other research where only an anthropogenic AOT is reported, we combine GOCART anthropogenic SU, OC, and BC components to provide comparison FMF and OMI-AI statistics. We make the assumption that the naturally occurring components of OC and BC are relatively small as they only contribute ~10% and 0% to the GOCART OC and BC AOT, respectively. For grid cells classified to an individual aerosol type, the pressure height of the maximum GOCART aerosol extinction

A reanalysis of MODIS fine mode fraction over ocean

T. A. Jones and
S. A. Christopher

Title Page

Abstract	Introduction
Conclusions	References
Tables	Figures

◄◄   ►►

◄   ►

Back   Close

Full Screen / Esc

Printer-friendly Version

Interactive Discussion

is calculated and compared with MODIS FMF and OMI-AI. Vertical aerosol distributions are assessed along with satellite observations to examine the relationship between aerosol height and the total-column statistics. The same methods are applied for CERES-SSF and MODIS L2 data from Aqua and Terra to compare the differences in sampling assumptions and observation time on the AOT and FMF averages for each individual aerosol type region.

The threshold level (80%) used to determine these regions was defined based on the work done by JC07 who showed that the variability in aerosol size properties for regions defined using 80% or higher thresholds was very low, being on the order of only a few percent. Higher thresholds were tested, but only reduced sample size while reporting almost identical statistics. However, these thresholds were only tested using GOCART simulations, and may require adjustment if other aerosol model simulations are considered. Over the oceans, the greatest uncertainty lies in the concentration and particle size properties of SS aerosols (Textor et al., 2006). If the simulated SS AOT were to be too high, this would require the use of lower thresholds to determine regions where other aerosol types such as DU, SU and BC exist. While the thresholds may differ, the resulting size and shape of the regions considered have good agreement given the greater certainty in the properties of the remaining aerosol types. If the regions are similar, then the corresponding satellite-derived statistics will also be similar to those presented by this study.

For comparison with previous research by Kaufman et al. (2005a,b) and Yu et al. (2009), we calculate the same FMF statistics using oceanic regions defined by these studies as being primarily associated with a single aerosol type. Their SS region lies in the Southern Hemisphere away from most DU or AN sources (20°–30° S; 50°–120° E) for the entire year (Fig. 1). Dust FMF values are obtained west of the North African coast (15° W–20° W; 15° N–20° N) between June and October, while AN values are obtained from the Western Atlantic (65° W–85° W (±5°); 40° N–50° N) for June and July data only (Kaufman et al., 2005a). Within these regions, aerosols type is assumed to be predominately SS, DU, or AN with spatial and temporal variations of aerosol

characteristics assumed to be small. Both Kaufman et al. (2005a,b) and Yu et al. (2009) used MODIS data from only the Terra satellite when computing their statistics.

4 Results

4.1 AOT and FMF statistics

The spatial distribution of various aerosol types in GOCART between June 2006 and May 2007 is clearly evident in Fig. 1. In this figure, each color represents the location where one or more daily $2.0 \times 2.5°$ grid cells is classified as SS, DU, CC, naturally and/or anthropogenic SU for each season using the 80% GOCART AOT threshold discussed in Sect. 3. (Organic and black carbon components are combined into a single carbon or CC type aerosol.) The fraction of total AOT from dust aerosols is greatest in the North Atlantic for all seasons due to mineral dust transported westward from the Saharan Desert. Anthropogenic SU regions occur off the eastern coasts of North America and China as well as surrounding Europe near where significant amounts of pollution are present. Naturally occurring SU, primarily from volcanic activity (Indonesia) are dominant in several locations in the Southern Hemisphere. CC associated with biomass burning contributes the greatest fraction to the total AOT west of Central Africa, while SS concentrations are mostly seen in the Southern Ocean south of 40° S, where average wind speeds are greater than over more tropical oceanic regions. The spatial extent and locations of these regions change significantly as a function of time due to changes in atmospheric transport, stability, and aerosol production (JC07) (Fig. 1). Standard deviations of GOCART FMF for all aerosol components in this research are less than ±0.05 indicating that the 80% threshold being used to define component specific regions is adequate for estimating individual aerosol type characteristics.

The mean MODIS AOTs at 0.55 μm within each grid cell from the Aqua CERES-SSF dataset are as follows, SS: 0.08±0.03, DU: 0.33±0.21, CC: 0.36±0.05, natural SU: 0.08±0.05, and anthropogenic SU: 0.17±0.05 (Table 2). *It is important to note*

that these and later FMF statistics are not global values, but only represent data within a particular aerosol component region as shown in Fig. 1. Aerosol concentrations are much higher in DU and CC regions compared to SS and SU regions, which is important since the lower the total aerosol concentration, the more uncertainty in aerosol component classifications exists. The mean FMF values for the Aqua CERES-SSF dataset are SS: 0.31±0.09 (f_{ss}), DU: 0.49±0.13 (f_{du}), CC: 0.80±0.16 (f_{cc}), natural SU: 0.69±0.20 (f_{nsu}), and anthropogenic SU: 0.77±0.16 (f_{asu}) between June 2006 and 2007 (Table 2). Corresponding values from the MYD04 dataset are SS: 0.34±0.11, DU; 0.46±0.14, CC: 0.77±0.17, natural SU 0.68±0.20, and anthropogenic SU: 0.74±0.15, which are similar to the CERES-SSF values (Table 1). Statistics computed using MOD04 L2 data from the Terra satellite showed some differences compared to the Aqua estimates, with f_{ss} being small and f_{cc} and f_{asu} being higher (Table 2). Reasons for these differences are explored further below. The standard deviation represents the yearly variability of all data in space and time classified as belonging to an individual aerosol type. These values should not be interpreted as uncertainties (e.g., Yu et al., 2009), but rather a measure of the variability in aerosol properties for individual aerosol types. As a result, these standard deviations are not necessarily comparable with uncertainty estimates reported by some other studies.

Overall variability is somewhat larger than reported by JC07 primarily due to the use of daily data in place of monthly averaged data. The distribution of MODIS FMF from the CERES-SSF product can be visualized in Fig. 2a, which shows the frequency distributions of FMF for the five aerosol types analyzed. Both f_{ss} and f_{du} have relatively normal distributions about the mean with the peak probability corresponding almost exactly with the mean value reported. As a result, regions being defined by GOCART as corresponding to either DU or SS appear have relatively uniform aerosol characteristics, and the FMF values agree well with those reported independently by Kaufman et al. (2005a,b) and JC07. Similar distributions were derived from MODIS L2 Aqua and Terra data over the same regions (Fig. 2b,c). However, in the case of Terra data, the maximum probabilities of SS and DU occur at lower FMF values (larger

A reanalysis of MODIS fine mode fraction over ocean

T. A. Jones and
S. A. Christopher

Title Page

Abstract	Introduction
Conclusions	References
Tables	Figures

|◄ | ►|
◄ | ►

Back | Close

Full Screen / Esc

Printer-friendly Version

Interactive Discussion

coarse mode component) while the maxima for other aerosol types occur at higher FMF values (larger fine-mode component), consistent with mean values shown in Table 1. For all satellite datasets, our estimates of FMF associated with anthropogenic aerosols (e.g. CC and SU) are consistently lower than some previous estimates. Recall that GOCART defines all SU and CC as fine mode; thus, f_{su} and f_{cc}=1.0. Kaufman et al. (2005a,b) and others have estimated FMF for these aerosol types to be approximately 0.9. Our estimates are approximately 0.1 lower, indicating a somewhat larger component of coarse mode aerosols in our regions compared to others. Further differences are also apparent when comparing the CERES-SSF CC and SU distributions to those from the MODIS L2 data from Aqua and Terra. Details of these differences and their potential causes are examined in further detail below for each aerosol type.

4.1.1 Sea salt

Good agreement exists between estimates of f_{ss} for the domains defined by Kaufman et al. (2005) for all datasets analyzed by this study (Table 1). Yu et al. (2009) estimates f_{ss} to be 0.45, which compares to an Aqua CERES-SSF value of 0.49 for the same area. MODIS L2 Aqua and Terra estimates are also similar (0.49, 0.50). The differences between these estimates are relatively small and within expected uncertainties, especially given the low overall SS AOT. However, the satellite estimates for f_{ss} using the GOCART defined regions are all less than 0.35, with the MODIS L2 Terra estimate being less than 0.3 (Table 1). Yu et al. (2009) noted a strong seasonal and spatial variability in SS particle size estimates, attributing them to changes in DMS and SS particle size as a function of wind speed. MODIS FMF values for marine aerosols during June, July, and August (JJA) ranged between 0.1 and 0.4 using their analysis technique over the Southern Ocean. However, it must also be noted that "marine" aerosols in Yu et al. (2009) include DMS and volcanic sulfates, which are not considered "marine" for the other methods referenced and employed by this study. In addition, the GOCART-defined SS region is not located anywhere near the region specified by Kaufman et al. (2005a).

A reanalysis of MODIS fine mode fraction over ocean

T. A. Jones and
S. A. Christopher

Title Page

Abstract	Introduction
Conclusions	References
Tables	Figures

|◄ | ►|
◄ | ►

Back | Close

Full Screen / Esc

Printer-friendly Version

Interactive Discussion

If we consider the region between 40° S and 60° S, MODIS AOT was lower and FMF was higher during SON and DJF than compared to the remainder of the season (Yu et al., 2009). However, the SS region derived in this study is small south of −40° S for DJF and also for JJA (Fig. 1). In JJA, the satellite viewing geometry thresholds reduce sampling below 40° S; thus, our SS statistics do not take into account aerosols further south during this season. For DJF, cloud clearing thresholds eliminate data over much of the same region. As a result, it stands to reason that our yearly averaged values correspond best with the values noted by Remer et al. (2008) and Yu et al. (2009) for the seasons for which the largest SS samples exist south of −40° S. Furthermore, changes in atmospheric humidity over space and time can also lead to changes sea-salt particle size. However, no significant differences in average total column RH were found between the GOCART and Kaufman et al. (2005a) SS regions during this one year period, and no significant correlation in monthly f_{ss} and RH was found for either sample. This is not to say that RH doesn't have an important effect on aerosol size. Rather, our analysis indicates other factors are more dominant when it comes to the variation in f_{ss} observed here. Also, note that the cloud-clearing thresholds used are likely removing the highest humidity regions, reducing hygroscopic effects from our sample. Our results show that estimates of f_{ss} from satellite observations are highly dependent on the spatial and temporal extent assumed when making these estimates. As suggested by Yu et al. (2009), it is clear that no single f_{ss} is representative of all sea-salt aerosols around the globe.

4.1.2 Dust

Comparing our results for f_{du} against those reported by Yu et al. (2009), GOCART simulations, and satellite data within regions specified by Kaufman et al. (2005), we find values generally between 0.3 and 0.45 (Table 1). Yu et al. (2009) reported a value of 0.37 with the corresponding GOCART values being 0.30 and slightly lower (0.27) if FMF is averaged over the larger DU region identified by this study (Fig. 1). The location of the Kaufman et al. (2005a) dust region lies within the GOCART region;

A reanalysis of MODIS fine mode fraction over ocean

T. A. Jones and
S. A. Christopher

thus, similar estimates between both methods would be expected. However, previous research such as Kaufman et al. (2005a,b) and JC07 report f_{du} closer to 0.5. Both Yu et al. (2009) and GOCART indicate the presence of a greater proportion of coarse mode aerosols than compared to these previous estimates. It should be noted that Kaufman et al. (2005a,b) used Collection 4 MODIS data, with later research using Collection 5 MODIS data (e.g., Yu et al., 2009). Improvements in aerosol property characterizations between Collection 4 and 5 reduced FMF values over the ocean between 20 and 50% depending on aerosol type (Remer et al., 2008).

Using the Aqua CERES-SSF dataset, our estimate for f_{du} is 0.49, higher than the GOCART model estimate (0.27) for the same region. Additional observations of DU from satellite data were made by Remer et al. (2008) who reported FMF values between 0.4 and 0.45 averaged for a larger area in the North Atlantic, which is not very different than the values reported here especially when considering that non-dust regions were not excluded from their regional average. However, when we compare the FMF values between MODIS L2 Terra and Aqua data, a significant difference in f_{du} becomes apparent (Table 1). The f_{du} estimate from Terra data is much lower than the corresponding Aqua estimates (0.36 vs. 0.46 and 0.49) for the GOCART defined DU region. This difference is also hinted using the Kaufman et al. (2005a) DU region where the f_{du} also is 0.36 for Terra data, but greater than 0.4 for both Aqua datasets (Table 1). Since the spatial and (daily) temporal sampling characteristics for the Terra and Aqua samples are quite similar, something else is likely causing these differences. One possibility is calibration differences between the two satellites, but previous studies have noted that if any difference does exist, it is relatively small and within expected uncertainties (Remer et al., 2008). Another possibility lies in diurnal variability of aerosol size distributions associated with individual aerosol types. Smirnov et al. (2002) noted that the diurnal variability of aerosol concentrations from AERONET data was generally less than 10% for dust aerosols, though did not report whether or not changes in aerosol size characteristics occurred. This variability may also be a function of changes in the vertical distribution of aerosols during the day even though the total

aerosol concentration remains unchanged. Atmospheric moisture content is unlikely to be the cause since dust aerosols are primarily hydrophobic in nature. Unfortunately, the current lack of high temporal resolution aerosol size and vertical distribution data from satellites makes further analysis of the question difficult.

4.1.3   Sulfates and carbonates

Additional differences between methods and datasets are apparent when comparing our FMF estimates of SU and CC against those from previous studies (Table 1). We estimate mean FMF values for anthropogenic (f_{asu}) and naturally occurring sulfate (f_{nsu}) to be 0.77 and 0.69 with the corresponding total carbonate value (f_{cc}) of 0.80 using the Aqua CERES-SSF dataset (Table 2). Results from the Aqua and Terra MODIS L2 datasets are similar, with Terra the combined anthropogenic (SU+CC) FMF values being somewhat higher (0.81 vs. 0.76). Modeling and observational studies have indicated that carbonates from African savanna burning are somewhat smaller in size than sulfates; thus, these aerosols should have slightly higher FMF estimates (e.g., Dubovik et al., 2002). The frequency distributions of both are much broader than for either SS or DU aerosols for all three datasets indicating a presence of multiple aerosol types in regions GOCART classifies as predominately fine mode (Fig. 2). Recall that GOCART defines all SU and CC as fine mode aerosols and does not consider internal mixing (Chin et al., 2002, 2004). Thus, there exists an apparent difference in FMF estimates between GOCART and satellite observations within the same regions. Part of this difference may also be due to coarse mode aerosols (either DU or SS) being present in small concentrations, but not being simulated by GOCART. Compared to DU and CC regions, AOT retrievals associated with anthropogenic and especially naturally occurring SU regions are much smaller (Table 2), leading to increased uncertainty in aerosol size estimates (Kleidman et al., 2005). Even small uncertainties in the coarse or fine mode components of AOT can have significant effects to observed FMF. Given the variability in SS aerosol properties from various aerosol models, the combination of a slight underestimate of SS AOT coupled with relatively low fine mode aerosol concentrations

could produce regions that contain a greater component of SS aerosols than would otherwise be the case. In this instance, FMF estimates for SU and CC regions would be lower, which is consistent with our observations.

The broad distributions in FMF for SU and CC aerosols are also partially a result of the update from Collection 4 to Collection 5 retrieval algorithms. Remer et al. (2005) showed a frequency distribution where a significant number of FMF observations of pollution aerosols lie between 0.4 and 0.6. Yu et al. (2009) used the same locations and methods used by Kaufman et al. (2005a) to derive their Collection 5 FMF estimates for AN aerosols, but aerosol characteristics over other geographical areas were not examined (Fig. 1). In particular, the Kaufman et al. (2005a) anthropogenic region is limited to a small region off the northeastern coast of the United States. It does not take into account anthropogenic or naturally occurring SU from South America, the Indian Ocean, or the Western Pacific. Similarly, they do not sample the characteristics of CC aerosols off the coast of Africa. Our method does take these additional areas into account, providing another potential reason for the difference in AN vs. SU and CC estimates reported here. When only the Kaufman et al. (2005a) region is sampled, the anthropogenic SU estimates between the two methods are the closest (0.87 vs. 0.90). However, if we apply these assumptions to the other SU and CC regions, then resulting radiative effect estimates may not be completely representative of all anthropogenic aerosols. Other potential reasons for these differences include using Level 2 vs. Level 3 MODIS data, the methods used to aggregate data to a particular grid, and different cloud clearing criteria.

4.1.4 Uncertainty in anthropogenic AOT

The importance of differences in aerosol component FMF values between methods and satellites to estimate anthropogenic aerosol radiative effects can be illustrated by plugging in the various estimates and uncertainties listed above into the equation for the anthropogenic component of AOT (τ_{an}) given by Eq. (1) (Kaufman et al., 2005a).

$$\tau_{an} = [(f - f_{du})\tau - (f_{ss} - f_{du})\tau_{ss}]/(f_{an} - f_{du}) \tag{1}$$

To compute differences in τ_{an} as a function of various FMF statistics, we assume a unit value for total AOT ($\tau=1$) and constant values for sea salt AOT ($\tau_{ss}=0.06$) and an observed FMF ($f=0.7$). Using the original Kaufman et al. (2005a) thresholds, the an-
thropogenic component of AOT is 0.55 (Table 3). However, this value increases to 0.61 when substituting the values from Yu et al. (2009) and increases even further to between 0.7 and 0.8 using the FMF values produced from this research. It should be noted that when using a temporally varying f_{ss}, Yu et al. (2009) actually show a reduction of 20% in the anthropogenic component of AOT compared to Kaufman
et al. (2005a). Overall, a variation in f_{an} by 0.1 results in a change in τ_{an} of approximately 0.2 when the total AOT is 1.0. This uncertainty increases further if aerosol size properties change as a function of space and time, which does occur (JC07; Yu et al., 2009). We must caution that the relationship between uncertainty in anthropogenic AOT and anthropogenic radiative effects are not necessary linear, but that assumption
is made here in order to give a first-order estimate of this relationship. To further reduce uncertainties in aerosol type classifications, further information is needed beyond that available only from the MODIS.

4.2 OMI-AI

We use the Aerosol Index (AI) derived from the OMI to assess UV-absorbing aerosols
such as DU and CC. OMI-AI for these aerosols are clearly positive (mean values being 0.95 and 0.79) and have a frequency distribution whose values are greater than those for SS and both natural and anthropogenic SU where mean AI is equal to 0.07 and −0.08, respectively (Table 2, Fig. 3). OMI-AI is somewhat smaller for CC than for DU, since the CC types includes a component of non-absorbing OC aerosols. By combining
MODIS FMF and OMI-AI, we can gain a better sense of aerosol speciation from a remote sensing perspective than from either sensor alone. Plotting OMI-AI against FMF from the Aqua CERES-SSF dataset reveals a good separation in the satellite-derived

A reanalysis of MODIS fine mode fraction over ocean

T. A. Jones and
S. A. Christopher

properties of the various aerosol types studied. An OMI-AI value of 0.5 separates the majority of SS and SU from DU and CC. Similar values were used by Bellouin et al. (2005, 2008) to separate absorbing from non-absorbing aerosols when estimating anthropogenic aerosol radiative effects. DU and the BC component of CC are UV absorbing and are often located higher in the atmosphere; thus, produce greater AI values. In Fig. 4a, the relationship between AI and MODIS AOT is also apparent with higher values of AI clearly corresponding to higher values of AOT, denoted by increasing symbol sizes. Comparing AI against FMF, it is evident that a combination of FMF and AI denote regions associated with either DU or CC aerosols. Similarly, for AI<0.5, SS and SU can be separated with most SS aerosols occurring when FMF<0.4. Also note that symbol sizes for both SS and SU are smaller, corresponding to lower overall aerosol concentrations compared to either DU or CC (Table 2). A significant portion of SU classified data points with MODIS FMF values lie between 0.4 and 0.6, indicating the presence of additional coarse mode aerosols beyond just fine mode SU.

Mean FMF values for each aerosol type from the Aqua CERES-SSF dataset are calculated separately for non-absorbing (AI<0.5) and absorbing (AI>0.5) samples (Table 4). As expected, most of the DU and CC samples are absorbing while over 95% of the SS and SU data fall within the non-absorbing sample. FMF estimates for non-absorbing SS and SU and absorbing DU are similar to those calculated from the combined sample with similar standard deviations. If we examine the few points where natural or anthropogenic SU have AI>0.5, we find a much reduced FMF estimate (f_{asu}=0.70 vs. 0.77 and f_{nsu}=0.55 vs. 0.69), indicating the AI threshold removes non-sulfate, coarse mode aerosols from the remaining SU sample (Table 4). While the overall estimate for f_{su} still did not change significantly, the overall distribution is more biased toward high FMF values than previously. Using the AI threshold also makes a significant difference when considering the CC sample. For absorbing CC, f_{cc} is 0.87 compared to an estimate of 0.74 for CC points where AI<0.5. Since CC aerosols include some component of absorbing BC, the FMF estimate of 0.87 should be a better estimate of overall CC aerosol characteristics.

4.3 Vertical distribution

We take this analysis one step further and compare the pressure height of the maximum aerosol concentration as defined by GOCART to the CERES-SSF FMF for different aerosol classifications (Fig. 4b). As expected, SS aerosols are concentrated near the surface with most data-points lying below the 900 hPa layer. The maximum concentration of CC aerosols occurs around 800 hPa (or 2 km above the sea-level), consistent with an increase in biomass burning in Central Africa. The greatest concentration of both anthropogenic and naturally occurring SU lie below 850 hPa, but some SU was also simulated to be above the 600 hPa layer. Above 700 hPa, the mean f_{asu} is only 0.65, significantly lower than for anthropogenic SU below this layer where f_{asu}=0.76. One common denominator of nearly all of SU data at all levels is low AOT ($\tau<0.3$).

The greatest concentration of dust layer heights derived from GOCART range between 950 and 700 hPa (or 0.5–3 km). Note that GOCART considers DU as surface sources; thus, the vertical transport must lift the dust up to the 4–5 km levels seen in observations (Chin et al., 2002, 2003). When AOT is greatest, the dust layer height is also maximized occurring between 600 and 500 hPa ($\sim$5 km), which is consistent with case study observations of dust over the North African coast (e.g., Christopher et al., 2009). Ongoing validation of the vertical distributions of aerosols within GOCART is underway, but as of yet is not complete. Thus, we refrain from any further quantitative analysis at this time, but it is clear that the aerosol layer height in combination with satellite remote sensing tools can be used in future aerosol classification algorithms.

5 Conclusions

The combination of MODIS and OMI satellite-based retrievals of aerosol properties coupled with GOCART simulated aerosol speciation provides a framework whereby satellite observations can be used to estimate the concentrations of individual aerosol types in the atmosphere. MODIS FMF values for aerosol types reported here are

A reanalysis of MODIS fine mode fraction over ocean

T. A. Jones and
S. A. Christopher

similar to those presented by JC07 with most differences being within observed uncertainties (±0.1). Computations across three different datasets (two from Aqua and one from Terra) show that SS contained the most coarse mode aerosols followed by DU, natural and anthropogenic SU, and finally CC, which is predominately fine mode. However, FMF estimates from Terra, especially for DU, are somewhat different than those from Aqua implying different sensor calibration, a diurnal variation in aerosol size characteristics, and/or sampling differences due to cloud cover changes between the Terra and Aqua overpass times. Since DU is hydrophobic, differences in atmospheric humidity are not likely to be the cause. We recommend that future research using MODIS FMF data to estimate component radiative effects use the FMF values corresponding to a specific satellite until the differences observed between the various datasets are better understood.

OMI-AI observations in conjunction with MODIS provide value added information content to distinguish between boundary layer aerosols such as SS and SU, and elevated, UV-absorbing aerosols such as DU and CC. Comparing FMF estimates between absorbing (AI>0.5) and non-absorbing (AI<0.5) samples shows that SU and CC values are very sensitive to this classification. Over 95% of SU points occur when AI<0.5 and for the few SU points where AI>0.5, FMF values are generally lower, indicating the presence of additional coarse mode aerosols within these areas. Similarly, when AI>0.5, CC has a much higher FMF value than the remaining points where AI<0.5 (0.84 vs. 0.74), showing that OMI-AI is quite useful in improving the discrimination between CC and other types of aerosols that may be present. Furthermore, SS and many SU aerosols are concentrated in the boundary layer while DU and CC aerosol concentrations are generally greatest several kilometers above the surface. Future research will apply these improved aerosol classification techniques to better quantify the aerosol radiative effects of individual aerosol types.

The use of daily GOCART simulations improves our confidence in the results compared to monthly analysis in JC07. The frequency distributions of FMF and AI for SS and DU aerosols are relatively uniform around the mean providing high confidence in

these sample values for all three datasets examined here. However, much broader distributions were observed for CC and especially SU, indicating greater uncertainty in observed statistics for these aerosol types. Regions defined as primarily SU likely have a somewhat larger component of coarse mode aerosols than the model indicates, reducing both natural and anthropogenic f_{su} estimates over that expected from other studies such as Kaufman et al. (2005a,b) and Yu et al. (2009). This may be due to uncertainties in the SS component of AOT within the GOCART model causing the SU and CC regions to incorporate too much background SS into their FMF estimates. Uncertainties in MODIS fine vs. coarse mode AOT retrievals for low aerosol concentrations may also play a role. The addition of AI thresholds increased the FMF estimate for both CC and SU aerosols by removing pixels where observations indicate a non-trivial component of AOT is a result of absorbing aerosols, consistent with model uncertainty Even with the large uncertainties associated with both natural and anthropogenic f_{su}, the difference between it and f_{cc} is large enough (>0.1) to be considered significant. Thus, combining both these aerosols types into a single "anthropogenic" classification may actually further increase downstream uncertainties. Given the magnitude of what small changes in FMF estimates can do to the "anthropogenic" component of AOT (and radiative forcing estimates), great care must be taken when assessing aerosol radiative forcing from a satellite remote sensing perspective.

A reanalysis of MODIS fine mode fraction over ocean

T. A. Jones and S. A. Christopher

Title Page

Abstract	Introduction
Conclusions	References
Tables	Figures

|◄ | ►|
◄ | ►

Back | Close

Full Screen / Esc

Printer-friendly Version

Interactive Discussion

References

Bellouin, N., Boucher, O., Haywood, J., and Reddy, M. S.: Global estimate of aerosol direct radiative forcing from satellite measurements, Nature, 438, 1138–1141, doi:10.1038/nature04348, 2005.

Bellouin, N., Jones, A., Haywood, J., and Christopher, S. A.: Updated estimate of aerosol direct radiative forcing from satellite observations and comparison against the Hadley Centre climate model, J. Geophys. Res., 113, D10205, doi:10.1029/2007JD009385, 2008.

Chin, M., Ginoux, P., Kinne, S., Torres, O., Holben, B., Duncan, B., Martin, R., Logan, J., Higurashi, A., and Nakajima, T.: Aerosol distributions and radiative properties simulated in the GOCART model and comparisons with observations, J. Atmos. Sci., 59, 461–483, 2002.

Chin, M., Ginoux, P., Lucchesi, R., Huebert B., Weber, R., Anderson, T., Masonis, S., Blomquist, B., Bandy, A., and Thornton, D.: A global aerosol model forecast for the ACE-Asia field experiment, J. Geophys. Res., 108(D23), 8654, doi:10.1029/2003JD003642, 2003.

Chin, M., Chu, D., Levy, R., Remer, L., Kaufman, Y., Hoblen, B., Eck, T., and Ginoux, P.: Aerosol distribution in the Northern Hemisphere during ACE-Asia: results from global model, satellite observations, and Sun photometer measurements, J. Geophys. Res., 109, D23S90, doi:10.1029/2004JD004829, 2004.

Chin, M., Diehl, T., Ginoux, P., and Malm, W.: Intercontinental transport of pollution and dust aerosols: implications for regional air quality, Atmos. Chem. Phys., 7, 5501–5517, doi:10.5194/acp-7-5501-2007, 2007.

Chin, M., Diehl, T., Dubovik, O., Eck, T. F., Holben, B. N., Sinyuk, A., and Streets, D. G.: Light absorption by pollution, dust, and biomass burning aerosols: a global model study and evaluation with AERONET measurements, Ann. Geophys., 27, 3439–3464, doi:10.5194/angeo-27-3439-2009, 2009.

Christopher, S. A. and Jones, T. A.: Satellite-based assessment of cloud-free net radiative effect of dust aerosols over the Atlantic Ocean, Geophys. Res. Lett., 34, L02810, doi:10.1029/2006GL027783, 2007.

Christopher, S. A. and Jones, T. A.: Short-wave aerosol radiative efficiency over the global oceans derived from satellite data, Tellus, 60B, 636–640, doi:080529042315537, 2008a.

Christopher, S. A. and Jones, T. A.: Sample bias estimation for cloud-free aerosol effects over global oceans, IEEE T. Geosci. Remote, 46(6), 1728–1732, 2008b.

Christopher, S. A., Zhang, J., Kaufman, Y. J., and Remer, L. A.: Satellite-based assessment of

A reanalysis of MODIS fine mode fraction over ocean

T. A. Jones and S. A. Christopher

Title Page	
Abstract	Introduction
Conclusions	References
Tables	Figures
◀◀	▶▶
◀	▶
Back	Close

Full Screen / Esc

Printer-friendly Version

Interactive Discussion

top of atmosphere anthropogenic aerosol radiative forcing over cloud-free oceans, Geophys. Res. Lett., 33, L15816, doi:10.1029/2005GL025535, 2005.

Christopher, S. A., Johnson, B., Jones, T. A., and Haywood, J.: Vertical and spatial distribution of dust from aircraft and satellite measurements during the GERBILS field campaign, Geophys. Res. Lett., 36, L06806, doi:10.1029/2008GL037033, 2009.

Dubovik, O., Holben, B. N., Eck, T. F., Smirnov, A., Kaufman, Y. J., King, M. D., Tanré, D., and Slutsker, I.: Variability of absorption and optical properties of key aerosol types observed in worldwide locations, J. Atmos. Sci., 59, 590–608, 2002.

Ginoux, P. and Torres, O.: Empirical TOMS index for dust aerosol: applications to model validation and source characterization, J. Geophys. Res., 108(D17), 4534, doi:10.1029/2003JD003470, 2003.

Gupta, P. and Christopher, S. A.: Seven year particulate matter air quality assessment from surface and satellite measurements, Atmos. Chem. Phys., 8, 3311–3324, doi:10.5194/acp-8-3311-2008, 2008.

Hsu, N. C., Herman, J. R., Gleason, J. F., Torres, O., and Seftor, C. J.: Comparisons of the TOMS aerosol index with Sun-photometer aerosol optical thickness: results and applications, J. Geophys. Res., 104(D6), 6269–6280, doi:10.1029/1998JD200086, 1999.

Jones, T. A. and Christopher, S. A.: MODIS derived fine mode fraction characteristics of marine, dust, and anthropogenic aerosols over the ocean, constrained by GOCART, MOPITT, and TOMS, J. Geophys. Res., 112, D22204, doi:10.1029/2007JD00897, 2007a.

Jones, T. A. and Christopher, S. A.: Statistical variability of top of atmosphere cloud-free shortwave aerosol radiative effect, Atmos. Chem. Phys., 7, 2937–2948, doi:10.5194/acp-7-2937-2007, 2007b.

Jones, T. A., Christopher, S. A., and Quaas, J.: A six year satellite-based assessment of the regional variations in aerosol indirect effects, Atmos. Chem. Phys., 9, 4091–4114, doi:10.5194/acp-9-4091-2009, 2009.

Kaufman, Y. J., Boucher, O., Tanré, D., Chin, M., Remer, L. A., and Takemura, T.: Aerosol anthropogenic component estimated from satellite data, Geophys. Res. Lett., 32, L17804, doi:10.1029/2005GL023125, 2005a.

Kaufman, Y. J., Koren, I., Remer, L. A., Tanré, D., Ginoux, P., and Fan, S.: Dust transport and deposition observed from the Terra-Moderate Resolution Imaging Spectroradiometer (MODIS) spacecraft over the Atlantic Ocean, J. Geophys. Res., D10S12, doi:10.1029/2003JD004436, 2005b.

A reanalysis of MODIS fine mode fraction over ocean

T. A. Jones and S. A. Christopher

Title Page

Abstract	Introduction
Conclusions	References
Tables	Figures

|◄ | ►|

◄ | ►

Back | Close

Full Screen / Esc

Printer-friendly Version

Interactive Discussion

Kleidman, R., O'Neill, N., Remer, L., Kaufman, Y., Eck, T., Tanré, D., Dubovik, O., and Holben, B.: Comparison of Moderate Resolution Imaging Spectroradiometer (MODIS) and Aerosol Robotic Network (AERONET) remote-sensing retrievals of aerosol fine mode fraction over ocean, J. Geophys. Res., 110, D22205, doi:10.1029/2005JD005760, 2005.

Levin, Z., Ganor, E., and Gladstein, V.: The effects of desert particles coated with sulfate on rain formation in the Eastern Mediterranean, J. Appl. Meteorol., 35, 1511–1523, 1996.

Loeb, N. G. and Manalo-Smith, N.: Top-of-atmosphere direct radiative effect of aerosols over global oceans from merged CERES and MODIS observations, J. Climate, 18, 3506–3526, 2005.

Remer, L. A., Kaufman, Y. J., Tanré, D., Mattoo, S., Chu, D. A., Martins, J. V., Li, R.-R., Ichoku, C., Levy, R. C., Kleidman, R. G., Eck, T. F., and Vermote, E.: The MODIS aerosol algorithm, products and validation, J. Atmos. Sci., 62, 947–973, 2005.

Remer, L. A., Kleidman, R. G., Levy, R. C., Kaufman, Y., Tanré, D., Mattoo, S., Martins, J., Ichoku, C., Koren, I., Yu, H., and Holben, B.: Global aerosol climatology from the MODIS satellite sensors, J. Geophys. Res., 113, D14S07, doi:10.1029/2007JD009661, 2008.

Seland, O., Iversen, T., Kirkevag, A., and Storelvmo, T.: On basic shortcomings of aerosol-climate interactions in atmospheric GCMs, Tellus, 60A, 459–491, doi:10.1111/j.1600-0870.2008.00318.x, 2008.

Smirnov, A., Holben, B. N., Eck, T. F., Slutsker, I., Chatenet, B., and Pinker, R. T.: Diurnal variability of aerosol optical depth observed at AERONET (Aerosol Robotic Network) sites, Geophys. Res. Lett., 29, 2115, doi:10.1029/2002GL016305, 2002.

Textor, C., Schulz, M., Guibert, S., Kinne, S., Balkanski, Y., Bauer, S., Berntsen, T., Berglen, T., Boucher, O., Chin, M., Dentener, F., Diehl, T., Easter, R., Feichter, H., Fillmore, D., Ghan, S., Ginoux, P., Gong, S., Grini, A., Hendricks, J., Horowitz, L., Huang, P., Isaksen, I., Iversen, I., Kloster, S., Koch, D., Kirkevåg, A., Kristjansson, J. E., Krol, M., Lauer, A., Lamarque, J. F., Liu, X., Montanaro, V., Myhre, G., Penner, J., Pitari, G., Reddy, S., Seland, Ø., Stier, P., Takemura, T., and Tie, X.: Analysis and quantification of the diversities of aerosol life cycles within AeroCom, Atmos. Chem. Phys., 6, 1777–1813, doi:10.5194/acp-6-1777-2006, 2006.

Torres, O., Bhartia, P. K., Herman, J. R., Ahmad, Z., and Gleason, K.: Derivation of aerosol properties from satellite measurements of backscattered ultraviolet radiation: theoretical basis, J. Geophys. Res., 103, 17099–17110, 1998.

Torres, O., Bhartia, P. K., Herman, J. R., Sinyuk, A., Ginoux, P., and Holben, B. N.: A long-term record of aerosol optical depth from TOMS observations and comparison to AERONET

measurements, J. Atmos. Sci., 59(3), 398–413, 2002.

Torres, O., Tansksnen, A., Veihelmann, B., Ahn, C., Braak, R., Bhartia, P. K., Veefkind, P., and Levelt, P.: Aerosols and surface UV products from Ozone Monitoring Instrument observations: an overview, J. Geophys. Res., 112, D24S47, doi:10.1029/2007JD008809, 2007.

Wang, J., Xia, X., Wang, P., and Christopher, S. A.: Diurnal variability of dust aerosol optical thickness and Angstrom exponent over dust source regions in China, Geophys. Res. Lett., 31, L08107, doi:10.1029/2004GL019580, 2004.

Weaver, C., Da-Silva, A., Chin, M., Ginoux, P., Dubovik, O., Flittner, D., Zia, A., Remer, L., Holben, B., and Watson, G.: Direct insertion of MODIS radiances in a global aerosol transport model, J. Atmos. Sci., 64, 808–826, 2007.

Yu, H., Kaufman, Y. J., Chin, M., Feingold, G., Remer, L. A., Anderson, T. L., Balkanski, Y., Bellouin, N., Boucher, O., Christopher, S., DeCola, P., Kahn, R., Koch, D., Loeb, N., Reddy, M. S., Schulz, M., Takemura, T., and Zhou, M.: A review of measurement-based assessments of the aerosol direct radiative effect and forcing, Atmos. Chem. Phys., 6, 613–666, doi:10.5194/acp-6-613-2006, 2006.

Yu, H., Chin, M., Remer, L. A., Kleidman, R., Bellouin, N., Blan, H., and Diehl, T.: Variability of marine aerosol fine-mode fraction estimates of anthropogenic aerosol component over cloud-free oceans from the Moderate Resolution Imaging Spectroradiometer (MODIS), J. Geophys. Res., 114, D10206, doi:10.1029/2008JD010648, 2009.

Zhang, J., Christopher, S. A., Remer, L. A., and Kaufman, Y. J.: Shortwave aerosol cloud-free radiative forcing from Terra, I: angular models for aerosols, J. Geophys. Res., D10(S23), D10S23, doi:10.1029/2004jd005008, 2005.

Zhang, J. and Reid, J. S.: MODIS aerosol product analysis for data assimilation: assessment of over-ocean level 2 aerosol optical thickness retrievals, J. Geophys. Res., 111, D22207, doi:10.1029/2005JD006898, 2006.

A reanalysis of MODIS fine mode fraction over ocean

T. A. Jones and S. A. Christopher

Title Page

Abstract	Introduction
Conclusions	References
Tables	Figures

◀◀ ▶▶

◀ ▶

Back Close

Full Screen / Esc

Printer-friendly Version

Interactive Discussion

Table 1. Comparison of aerosol type FMF estimates from this research with those reported from previous studies where applicable. The term "anthropogenic" represents the combination of anthropogenic sulfates and all carbonates. FMF values in parenthesis indicate average FMF values for CC, NSU, and ASU aerosol components, where available. All uncertainty estimates for this research represent the standard deviation of FMF within a particular aerosol component region. Results from the Aqua Collection 5 CERES-SSF and MYD04 as well as Terra MOD04 products are shown.

	Sea-salt	Dust	Anthro	(CC, NSU, ASU)
Previous research				
Kaufman et al. (2005a)	0.30±0.10	0.50±0.05	0.90±0.05	
Kaufman et al. (2005b)	0.32±0.07	0.51±0.05	0.92±0.03	
Bellouin et al. (2005)	0.35±0.05	NA	0.83±0.05	
JC (2007)	0.25±0.09	0.44±0.06	0.83±0.04	
Yu et al. (2009)	0.45±0.05	0.37±0.05	0.90±0.05	
Kaufman boxes				
GOCART	0.43±0.04	0.30±0.06	0.83±0.09	
MOD04 C5 (Terra)	0.49±0.25	0.36±0.15	0.84±0.16	
MYD04 C5 (Aqua)	0.50±0.21	0.40±0.16	0.83±0.14	
CERES-SSF C5 (Aqua)	0.49±0.20	0.45±0.16	0.87±0.13	
This research				
GOCART	0.44±0.04	0.27±0.02	0.98±0.01	(0.99, 0.99, 0.97)
MOD04 C5 (Terra)	0.25±0.12	0.37±0.15	0.81±0.16	(0.81, 0.74, 0.81)
MYD04 C5 (Aqua)	0.34±0.11	0.46±0.14	0.76±0.18	(0.77, 0.86, 0.74)
CERES-SSF C5 (Aqua)	0.31±0.09	0.49±0.13	0.78±0.16	(0.80, 0.69, 0.77)

Full Screen / Esc

Printer-friendly Version

Interactive Discussion

Table 2. Yearly averaged GOCART AOT and FMF (GAOT, GFMF); sample size, AOT and FMF (AOT, FMF), and OMI-AI for sea-salt, dust, sulfates, and organic+black carbon between June 2006 and May 2007 for the Aqua CERES-SSF dataset.

Aerosol	GAOT	GFMF	NUM	AOT	FMF	OMI-AI	Pressure
Sea Salt	0.088	0.449	487	0.08±0.03	0.31±0.09	0.14±0.3	920±36
Dust	0.657	0.267	1280	0.33±0.21	0.49±0.13	0.95±0.5	839±85
A-Sulfate	0.279	0.967	296	0.17±0.08	0.77±0.16	−0.08±0.3	846±91
N-Sulfate	0.306	0.986	627	0.08±0.05	0.69±0.20	0.07±0.2	819±78
Carbon	0.490	0.991	335	0.36±0.29	0.80±0.16	0.79±0.6	825±83

Table 3. Anthropogenic AOT (τ_{an}) derived using the FMF statistics from Kaufman et al. (2005a), Yu et al. (2009), and our Aqua and Terra estimates. Assumptions include an observed unit AOT (τ=1.0), an observed FMF of 0.7 and a constant sea salt AOT of 0.06.

	τ_{an}
Previous research	
Kaufman et al. (2005a)	0.53
Yu et al. (2009)	0.61
This research	
MOD04 C5 (Terra)	0.69
MYD04 C5 (Aqua)	0.82
CERES-SSF C5 (Aqua)	0.76

Table 4. Aqua CERES-SSF sample size (NUM) and mean FMF values for OMI-AI<0.5 and OMI-AI>0.5 samples showing the influence of UV-absorbing aerosols on the resultant statistics. Note that significant differences appear when comparing SU and CC samples where the FMF for absorbing CC is much greater than the non-absorbing samples and the non-absorbing FMF for SU is greater than the absorbing sample.

Aerosol	AI<0.5 NUM	FMF	AI>0.5 NUM	FMF	ALL NUM	FMF
Sea salt	453	0.29±0.09	34	0.28±0.06	487	0.29±0.09
Dust	230	0.54±0.14	1050	0.49±0.12	1280	0.49±0.13
A-sulfate	291	0.77±0.20	5	0.70±0.17	296	0.77±0.16
N-sulfate	608	0.69±0.20	19	0.55±0.20	627	0.69±0.20
Carbon	120	0.74±0.18	215	0.84±0.14	335	0.80±0.16
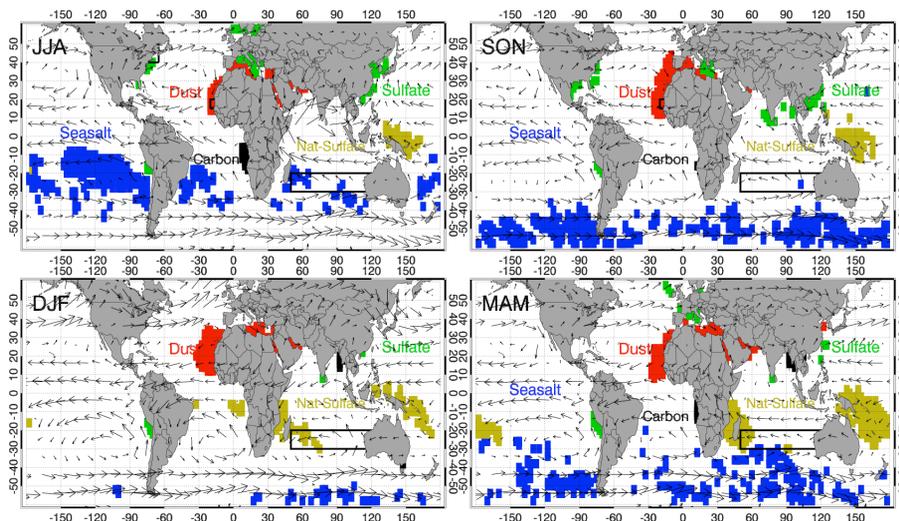
Fig. 1. Global aerosol distributions where at least 80% of the total GOCART AOT is represented by a single aerosol type (sea-salt, dust, natural sulfate, anthropogenic sulfate, or organic+black carbon) over the ocean between June 2006 and May 2007 for June, July, and August (JJA); September, October, and November (SON); December, January, and February (DJF); and March, April, and May (MAM). Black boxes show the regions defined by Kaufman et al. (2005a) corresponding to individual aerosol types (SS: west of Australia, DU: west of Africa, and AN: northeast of the United States). Vectors indicate the seasonally averaged 850-hPa wind speed and direction.
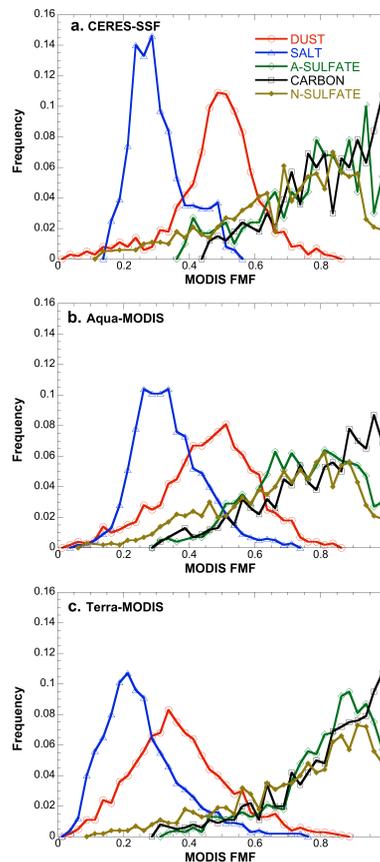
Fig. 2. (a) Frequency distribution of FMF values from the CERES-SSF dataset for 0.025 bins where at least 80% of the total GOCART AOT is from an individual aerosol type. Both SS and DU have relatively uniform distributions around their mean values (0.31, 0.49). MODIS L2 Aqua and Terra data from the same time period are shown in panels **(b)** and **(c)**, respectively.

Title Page

Abstract | Introduction

Conclusions | References

Tables | Figures

◄ | ►

◄ | ►

Back | Close

Full Screen / Esc

Printer-friendly Version

Interactive Discussion
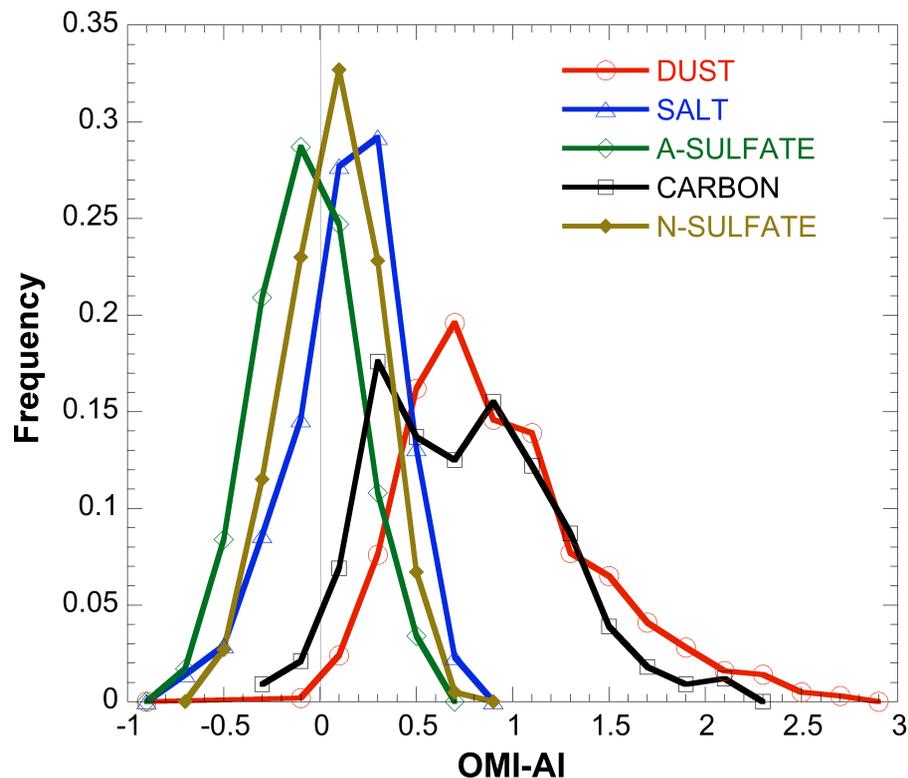
Fig. 3. Frequency distribution of OMI-AI for each aerosol type. Note that the AI frequency distribution of DU and CC is displaced to the right (more positive) of the other aerosol types.
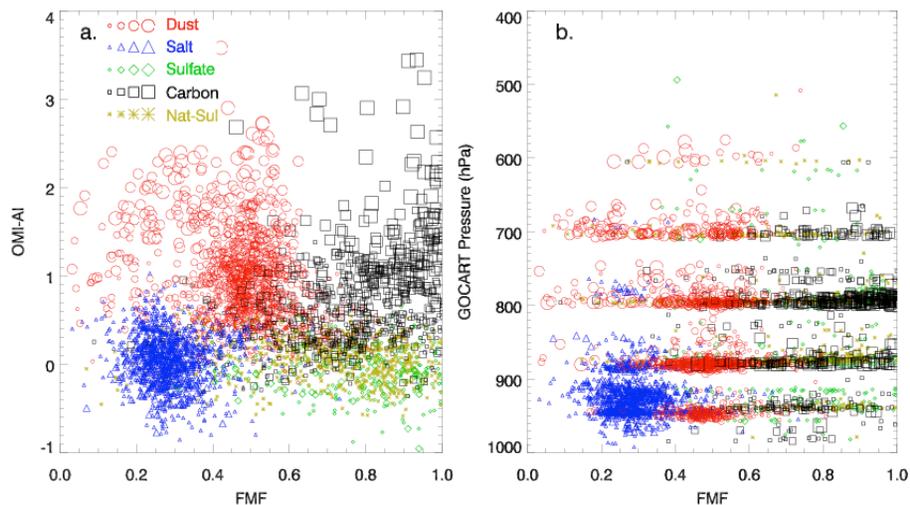
Fig. 4. (a) OMI-AI as a function of MODIS FMF color-coded by aerosol type, with increasing symbol sizes representing larger MODIS AOT in bins of (0.0<0.3; 0.3<0.6; 0.6<0.9; and AOT>0.9). **(b)** Scatter plot of the GOCART pressure height (hPa) of the maximum aerosol concentration as a function of MODIS FMF using same coloring and symbol size labels.